Available online at www.sciencedirect.com
SCIENCE DIRECT®
Computers and Structures 82 (2004) 281–299
Computers & Structures
www.elsevier.com/locate/compstruc

Optimization of mass concrete construction using genetic algorithms

Eduardo M.R. Fairbairn *, Marcos M. Silvoso, Romildo D. Toledo Filho, José L.D. Alves, Nelson F.F. Ebecken

Department of Civil Engineering, COPPE/Universidade Federal do Rio de Janeiro, CP 68506, CEP: 21945-970 Rio de Janeiro, RJ, Brazil

Received 24 January 2003; accepted 26 August 2003

Abstract

This paper presents a procedure to optimize the construction of mass concrete structures using genetic algorithms. The optimization criterion is construction cost and the decision variables are material types, placing temperature, the height of lifts and time intervals between lifts. The constraint imposed on the decision variables is cracking. Transient hydration, thermal and stress fields were calculated using a coupled thermo-chemo-mechanical model. To show the potential of the proposed methodology, the construction phase of a small hydropower plant dam was optimized. The results indicated that the procedure can be successfully used in the design of massive concrete structures.
© 2003 Elsevier Ltd. All rights reserved.

Keywords: Mass concrete; Hydration reaction; Autogenous shrinkage; Thermal stress; Early age cracking; Numerical modeling; Optimization; Genetic algorithms

1. Introduction

Massive concrete structures such as dams, foundation slabs and bridge decks may be subject to early age cracking due to thermal stresses and autogenous shrinkage-induced stresses [1,2]. From the engineering point of view, if cracking must be avoided, several measures can be undertaken to reduce the early effects of the hydration reaction [3–7], such as:

(a) choosing a material composition that gives lower rates of hydration and/or limiting the autogenous shrinkage potential;
(b) controlling lift thickness and the time intervals between lifts to allow heat to dissipate;
(c) reducing the placing temperature of concrete, or using pipecooling.

All of these measures involve costs, and it is up to the engineer to decide which measure, or which combination of measures, is the optimal one, considering that construction cost should be minimized without compromising the safety and durability of the construction.

Traditionally, this optimization problem has been solved through the know-how of the structural design team, using more or less sophisticated numerical models [8–12]. However, mass concrete construction involves extremely large volumes of concrete and significant manpower. For example, the Itumbiara dam in Brazil, with an installed capacity of 2.1 GW required about 2 million m^3 of concrete, cooled before placing, and thousands of workers for its construction [13]. In order to control temperature increases in mass constructions, part of the cement in the concrete mix is often replaced by pozzolanic materials. While the decision on the blend of cementitious material will determine the extent and kinetics of the hydration reaction, it also depends on the cost/benefit relationship of blending the cementitious material.

* Corresponding author. Tel.: +55-21-560-8993; fax: +55-21-256-28484.
E-mail address: eduardo@coc.ufrj.br (E.M.R. Fairbairn).

0045-7949/$ - see front matter © 2003 Elsevier Ltd. All rights reserved.
doi:10.1016/j.compstruc.2003.08.008

Because of the large volume of concrete and the logistics involved in construction of massive structures, an accurate and feasible procedure that could be used consistently to optimize the variables intervening in mass concrete construction would be very helpful to both the designer and the contractor.

An extensive 1998 survey on Cost Optimization of Concrete Structures [14] showed that the great majority of papers dealing with structural optimization concerned weight minimization. Of the small number of papers on cost optimization, most were dedicated to simple elements such as beams and girders, and very few used costs functions that considered the costs of placement and construction. Since 1998, the panorama has not essentially changed and no reference on the optimization of mass concrete structures was found, although mass concrete cost optimization can result in substantial savings.

This paper presents a procedure for optimizing the construction phase of mass concrete structures. This is a cost optimization problem that involves the cost of the raw material and construction costs associated with placing, cooling, formwork, lift height and time intervals.

The procedure presented in this paper systematizes the cost optimization problem of mass concrete construction using:

(i) a coupled thermo-chemo-mechanical model (Ulm and Coussy [15,16]) implemented in a 3D FEM code [17] to simulate the effects of the hydration reaction;
(ii) a genetic algorithm procedure [18] to optimize construction costs.

Ulm and Coussy's thermo-chemo-mechanical model was chosen because of its soundness and feasibility for engineering applications. For example, the model proved to be accurate in the early age analysis and design of tunnel platforms made of steel-fiber reinforced high performance concrete for the French TGV [19], the analysis of the fire in the Channel Tunnel that connects England and France [20] and the analysis of early age cracking in shotcrete tunnel shell construction [21].

The parameters necessary for implementation of Ulm and Coussy's model are easily obtained by means of experimental tests that are commonly performed for mass concrete construction, such as adiabatic or semi-adiabatic temperature evolution, compressive strength and (less frequently) autogenous shrinkage.

In genetic algorithms, structural design optimization problems have three main characteristics [22]: (i) the solution sought is the global optimal solution, (ii) design variables are generally discrete variables and (iii) structural design optimization always contains constraints. Genetic algorithms provide effective solutions to discrete optimization problems, search for the global optimal point and can be modified to incorporate constraints. For these reasons, genetic algorithms have gained widespread acceptance, and several applications in structural design optimization have been reported in the last few years. We make reference to a few recent journal papers on: optimal design of planar and space steel frames [23–25]; optimization of space and planar trusses [26–29]; continuum structural topology design [30]; optimum rigid pavement design [31]; location of damage in structures [32]; design of composite structures [33]; and topology optimization of shells [34].

The potential of the procedure presented in this paper is demonstrated through the optimization of the construction phase of a concrete dam for a small hydropower plant. The results indicate that the proposed procedure is both accurate and feasible and should become a useful tool for optimizing mass concrete construction.

2. Ulm and Coussys thermo-chemo-mechanical model

2.1. Evolution of the hydration reaction

The Ulm and Coussy's model considers concrete as a reactive porous media composed of a solid skeleton of anhydrous cement grains and CSH hydrates and pores that may be filled by either air or water.

The evolution of the hydration reaction is represented by an Arrhenius-type equation, which takes into account the thermo-activation and exothermic nature of the reaction:

$$\frac{\mathrm{d}m}{\mathrm{d}t} = \frac{\mathrm{d}\xi}{\mathrm{d}t} m_\infty = \frac{1}{\eta(\xi)} A(\xi) \exp\left(-\frac{E_a}{RT}\right) \tag{1}$$

where $\mathrm{d}m/\mathrm{d}t$ is the variation of the skeleton mass; $0 < \xi < 1$ is the degree of hydration or, in other words, the relation between the mass of the skeleton at a time t normalized by the mass of the skeleton when hydration is complete, i.e., $\xi(t) = m(t)/m_\infty$; $\eta(\xi)$ is a viscosity term representing the increase in physical barrier of CSH, which tends to isolate the cement grain from the free water and depends on the state of the hydration reaction; $A(\xi)$ is the affinity of the chemical reaction or, in other words, the thermodynamic force associated to the rate of hydrates formation, which also depends on the state of the hydration reaction; E_a is the apparent thermal activation energy, which is considered to be constant with relation to the hydration degree; R is the universal constant of gases; and T is the temperature in Kelvin.

2.2. Thermo-chemical coupling

The equation for the transient thermal and hydration fields that compose the thermo-chemical coupling is:

$$C_\varepsilon \dot{T} = Q + L\dot{\xi} + k\nabla^2 T \tag{2}$$

Here, the standard form for evolution of thermal fields, $C_\varepsilon \dot{T} = Q + k\nabla^2 T$, can be recognized, with C_ε being the specific heat and k the thermal conductivity. The term $L\dot{\xi}$ represents the heat generated by the exothermic reaction, with L being the latent heat of hydration determined by means of experimental tests.

Eq. (2) can have a step-by-step solution if the values of $\dot{\xi}$ (and consequently the values of ξ) are determined, for each time-step, by means of Eq. (1). For this purpose it is necessary to know the values of the normalized affinity $\widetilde{A}(\xi) = A(\xi)/(m_\infty \eta(\xi))$. This may be obtained by means of either adiabatic or quasi-adiabatic tests.

2.3. Chemo-mechanical coupling

The chemo-mechanical coupling is represented by the following equation:

$$\mathrm{d}\boldsymbol{\sigma} = \mathbf{C}(\xi) : (\mathrm{d}\boldsymbol{\varepsilon} - \mathrm{d}\boldsymbol{\varepsilon}^{\mathrm{p}} - \alpha_{\mathrm{T}}\mathbf{1}\,\mathrm{d}T - \beta(\xi)\mathbf{1}\,\mathrm{d}\xi) \tag{3}$$

where $\boldsymbol{\sigma}$ is the stress tensor; $\mathbf{C}(\xi)$ is the elastic compliance tensor dependent on the degree of hydration (because Poisson's ratio v is considered to be constant with the degree of hydration, we can say that $\mathbf{C}(\xi) = \mathbf{C}(E(\xi))$); $\boldsymbol{\varepsilon}^{\mathrm{p}}$ is the plastic strains tensor; $\boldsymbol{\varepsilon}$ is the strain tensor; α_{T} is the thermal dilatation coefficient, considered to be constant for the temperature range of the problem at hand; $\mathbf{1}$ is the identity tensor; $\beta(\xi)$ is the coefficient relating the hydration rate to the autogenous shrinkage; and the operator **:** indicates the scalar product of two tensors.

2.4. Chemo-plastic coupling

In this paper we use multi-surface plasticity as described by Simo and Hughes [35] and implemented by Ferreira [36] and Helmich [37]. The chemo-plastic coupling considers that the hardening forces $\boldsymbol{\zeta}$, which are associated with the sizes of the yield surfaces in the stress space, depend on both the plastic hardening/softening variables $\boldsymbol{\chi}$ and the evolution of the hydration reaction ξ, reading, formally, $\boldsymbol{\zeta}(\boldsymbol{\chi}, \xi)$. Two yield surfaces are employed, namely, *Drucker–Prager* when the stress state is of the compressive type, and *tension-cut-off* when the stress state is of the tension type. Within the framework of associative plasticity, one can write the flow and the hardening rules as follows:

$$\mathrm{d}\boldsymbol{\varepsilon}^{\mathrm{p}} = \sum_{s \in J_{\mathrm{act}}} \mathrm{d}\lambda_{\mathrm{S}} \frac{\partial f_{\mathrm{S}}}{\partial \boldsymbol{\sigma}} \tag{4}$$

$$\mathrm{d}\chi_1 = \mathrm{d}\lambda_1 \frac{\partial f_1}{\partial \zeta_1}; \qquad \mathrm{d}\chi_2 = \mathrm{d}\lambda_2 \frac{\partial f_2}{\partial \zeta_2} \tag{5}$$

where J_{act} is the set of active surfaces, i.e., the surfaces for which $f_{\mathrm{S}}(\boldsymbol{\sigma}, \boldsymbol{\zeta}) = 0$; and $\mathrm{d}\lambda_{\mathrm{S}}$ are plastic multipliers, defined as in standard plasticity [35].

Given that only the Drucker–Prager criterion allows for hardening, the two criteria used in this paper, represented by the functions f_1 and f_2 can be written as:

$$\begin{aligned} &f_1 = \alpha(I_1 + 3\zeta_1(\chi_1, \xi)) + J_2^{1/2} \leqslant 0 \\ &\alpha = \frac{1}{\sqrt{3}} \frac{\kappa - 1}{2\kappa - 1} \end{aligned} \tag{6}$$

$$f_2 = I_1 + 3\zeta_2(\xi) \leqslant 0 \tag{7}$$

where $I_1 = \mathrm{tr}(\boldsymbol{\sigma})$ and $J_2 = (\boldsymbol{s} : \boldsymbol{s})/2$ are, respectively, the first invariant of the stress tensor and the second invariant of the deviatoric stress tensor and $\kappa = f_{\mathrm{b}}(\xi)/f_{\mathrm{c}}(\xi)$ is the ratio between the biaxial and the uniaxial compressive strengths, considered to be constant ($\kappa = 1.16$) with hydration.

2.5. Evolution laws

2.5.1. Compressive and tensile strengths

The relationship between compressive strength and the degree of hydration is bilinear, as shown below [38]:

$$\begin{aligned} &f_{\mathrm{c}}(\xi) = 0 \quad \text{for } \xi < \xi_0, \quad \text{and} \\ &f_{\mathrm{c}}(\xi) = f_{\mathrm{c},\infty}[(\xi - \xi_0)/(1 - \xi_0)] \quad \text{for } \xi \geqslant \xi_0 \end{aligned} \tag{8}$$

where $f_{\mathrm{c},\infty} = f_{\mathrm{c}}(\xi = 1)$ is the compressive strength where hydration is complete; and ξ_0 is the degree of hydration at the percolation threshold, defined by Acker [39] as the very moment when concrete becomes a solid. The tensile strength $f_{\mathrm{t}}(\xi)$ is determined from the formulas (8), taking the ratio $f_{\mathrm{t}}(\xi)/f_{\mathrm{c}}(\xi) = 0.1$ to be constant with hydration.

2.5.2. Young's modulus

Byfor's law [40] is used to describe the relationship between Young's modulus and the degree of hydration:

$$E(\xi) = E_\infty \frac{1 + 1.37(f_{\mathrm{c},\infty})^{2.204}}{1 + 1.37(f_{\mathrm{c}}(\xi))^{2.204}} \left(\frac{f_{\mathrm{c}}(\xi)}{f_{\mathrm{c},\infty}} \right)^{2.675} \tag{9}$$

where $E_\infty = E(\xi = 1)$ is Young's modulus at complete hydration.

2.5.3. Autogenous shrinkage

The relationship between the hydration rate and autogenous shrinkage (see Eq. (3)) is bilinear:

$$\begin{aligned} &\beta(\xi) = 0 \quad \text{for } \xi < \xi_0, \quad \text{and} \\ &\beta(\xi) = \varepsilon_\infty^{\mathrm{sh}}/(1 - \xi_0) \quad \text{for } \xi \geqslant \xi_0 \end{aligned} \tag{10}$$

$\varepsilon_\infty^{\mathrm{sh}}$ being autogenous shrinkage at complete hydration, i.e., $\varepsilon_\infty^{\mathrm{sh}} = \varepsilon^{\mathrm{sh}}(\xi = 1)$.

2.5.4. Plastic variables

The evolution of the *Drucker–Pragger* and *tension-cut-off* surfaces, characterized by the hardening forces $\boldsymbol{\zeta}(\boldsymbol{\chi}, \xi)$, is given by the following equations:

$$\zeta_1(\chi_1, \xi) = \frac{\kappa}{3(1-\kappa)}\left[f_c(\xi)\varsigma + f_c(\xi)(1-\varsigma)\left(1 - \frac{(\chi_1 - \chi_{1,u})^2}{\chi_{1,u}^2}\right)\right]$$

for $\chi < \chi_{1,u}$

$$\zeta_1(\chi_1, \xi) = \frac{\kappa}{3(1-\kappa)} f_c(\xi) \quad \text{for } \chi_1 \geqslant \chi_{1,u};$$

$$\chi_{1,u} = \frac{9\alpha\left(f_{c,\infty} - E_\infty \varepsilon^u_{c,\infty}\right)}{E_\infty(3\alpha - \sqrt{3})} \tag{11}$$

$$\zeta_2(\xi) = -\frac{f_t(\xi)}{3} \tag{12}$$

where $\varsigma = f_y(\xi)/f_c(\xi)$ is the ratio between the yield stress and the compressive strength, which is assumed to remain constant during hydration ($\varsigma = 0.25$), and $\varepsilon^u_{c,\infty}$ is the ultimate value of uniaxial compressive strain associated with $f_{c,\infty}$, i. e., $\varepsilon^u_{c,\infty} = \varepsilon^u_c(\xi = 1)$.

3. Computational implementation

The model was implemented in a 3D FEM code. It uses linear tetrahedral elements and the non-linear system of equations is solved by using a Newton–Raphson incremental iterative technique. An element-by-element strategy solution with a preconditioned conjugate gradient solver and a diagonal preconditioner of the elements' matrices was used [50]. The code has two modules: the first module computes the transient thermal and hydration fields; the second module calculates the stresses and strain fields for each time-step.

To simulate the construction process, each element is associated to a construction phase and consequently to the activation time of that phase of the structure. When the activation time is reached, the corresponding finite elements are activated and the boundary conditions are updated. The data structure of the computer code and the element-by-element solution improve the efficiency of the numerical analysis and make the simulation of the construction phases easier. Details of the computational implementation can be seen in [17].

4. Genetic algorithms for the optimization of mass concrete construction

4.1. Genetic algorithm

The genetic algorithm used in this paper is based on the algorithm developed by Castro [18]. It is a generational algorithm with elitism of the best individual, tournament selection scheme, single point crossover and mutation genetic operators.

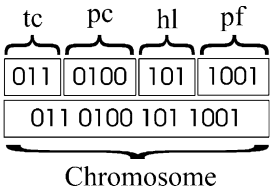

Fig. 1. Binary representation of the chromosome.

The control parameters are the population size (N), the crossover probability (P_c), the mutation probability (P_m), and the tournament size for tournament selection (N_t).

The design variables are encoded as binary strings that compose the chromosome (or individual), where each bit represents the chromosome's genes, as displayed in Fig. 1.

The population size (N) indicates the number of chromosomes for each generation, which is considered to be constant during the evolution process. It should be large enough to guarantee the diversity of the population, although the simulation will run more slowly if a large population is used. The initial population is chosen randomly to obtain maximum diversity. The selection of progenitors for the descendent generation is inspired by Darwin's evolutionary theory, where the fittest individuals are more likely to be selected to transmit their genes. Generally, the pairs of individuals are directly selected for reproduction from the population and their offspring will constitute the next generation.

Although several selection schemes can be found in the bibliography [41], in this paper the biologically inspired tournament selection method is used. It consists of two basic steps: (i) a set of N_t ($N_t \geqslant 2$) individuals is randomly selected from the population; and (ii) a tournament is carried out and the fittest individual is selected to reproduce. The tournament selection is then repeated as many times as necessary to find the total set of parents that will procreate the next generation.

The tournament selection method helps prevent stagnation and does not use rank ordering or any other extra procedure that would introduce an additional computational effort. Together with tournament selection, elitism is used to ensure that the best performing chromosome survives to the next generation.

The selected individuals will be paired randomly to procreate and crossover will be carried out with a crossover probability P_c. Thus, if a pair is selected to procreate, the genetic operator will create two new individuals from the genetic material of the selected parents. Otherwise, the two parents are repeated in the next generation. The one-point crossover operator shown in

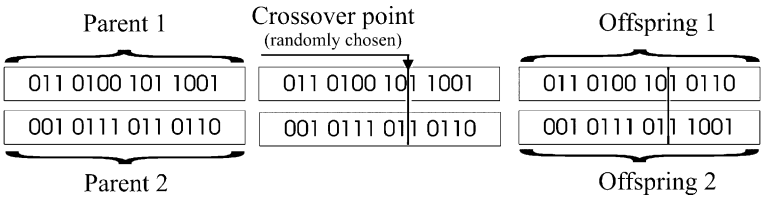

Fig. 2. One-point crossover operator.

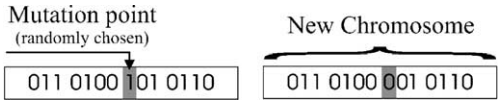

Fig. 3. *Bitflip* mutation operator.

Fig. 2, which mixes the genes of two parents using a randomly chosen point on the chromosome, is used.

The genetic diversity of the new population is ensured by the application of the mutation operator, applied with a small probability P_m. We use the *bitflip* mutation, which produces a minor perturbation in the chromosome, changing one randomly selected gene, as depicted in Fig. 3.

A general sketch of the genetic algorithm used in this paper is presented in the form of a flowchart in Fig. 4. The algorithm is terminated when the maximum number of generations (N_g) is achieved.

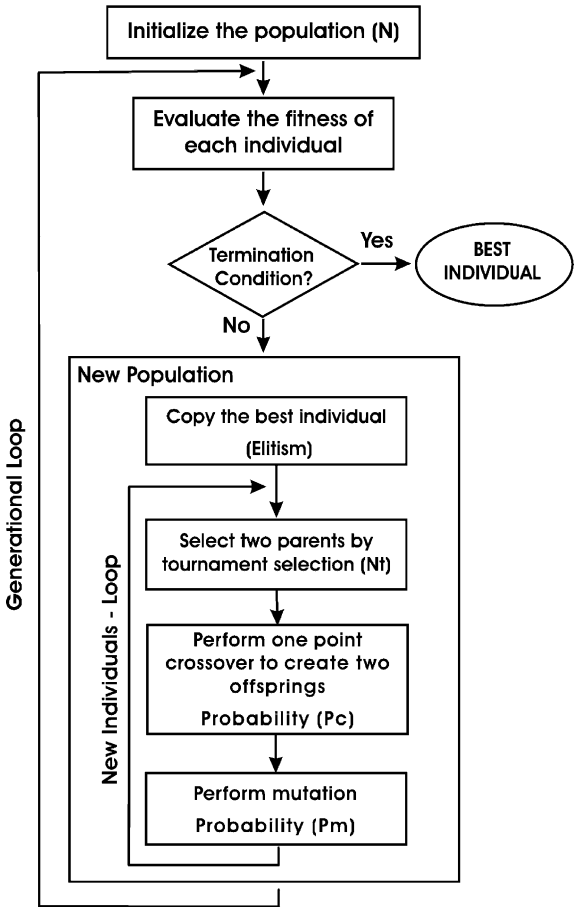

Fig. 4. Flowchart of the genetic algorithm.

4.2. Design variables

Within the framework of the methodology proposed in this paper, the design variables considered for the optimization of massive concrete structures are:

The type of concrete (tc). The choice of the material is directly related to the evolution of the hydration reaction (heat generation, autogenous shrinkage) and to the development of the properties of the skeleton such as the strength, Young's modulus and plastic properties. In general, the better the performance of the material, the greater is its cost. The type of concrete is a discrete variable, reading:

$$\mathrm{tc} \in \{1, 2, \ldots, N_{\mathrm{tc}}\} \tag{13}$$

where N_{tc} is the number of types of concrete. The variable tc is actually a pointer to the parameters that define the concrete's thermo-chemo-mechanical behavior (i.e., $C_\varepsilon(\mathrm{tc})$, $k(\mathrm{tc})$, $E_a(\mathrm{tc})$, $\alpha(\mathrm{tc})$, $f_{c,\infty}(\mathrm{tc})$, $E_\infty(\mathrm{tc})$, $\varepsilon_\infty^{sh}(\mathrm{tc})$, $\xi_0(\mathrm{tc})$) and to the composition of the concrete Comp(tc).

The composition of the concrete is expressed by:

$$\mathrm{Comp}(\mathrm{tc}) = \{B_{1,\mathrm{tc}}, B_{2,\mathrm{tc}}, \ldots, B_{n_B,\mathrm{tc}}, W_{\mathrm{tc}}, G_{1,\mathrm{tc}}, G_{2,\mathrm{tc}}, \ldots, G_{n_G,\mathrm{tc}}, A_{1,\mathrm{tc}}, A_{2,\mathrm{tc}}, \ldots, A_{n_A,\mathrm{tc}}\} \tag{14}$$

where the B, W, G and A represent, respectively, the mass content of binders such as cement, silica fume, fly ash, and slag (n_B being the number of binders); water; aggregates (n_G being the number of aggregates types); and chemical additives (n_A being the number of additives).

The placing temperature (pt). Since the hydration reaction is thermo-activated, cooling the concrete will help slow down the chemical reaction and reduce the risk of cracking. The two main practices commonly used

are precooling the material before placing and pipe cooling the material during curing. In this paper, pipe cooling is not considered and the variable related to cooling the material is the placing temperature. The variable pt is generally a discrete variable, since in most cases the costs corresponding to cooling the concrete will not be as exact as fractions of Celsius degrees. The variable can then be defined by taking its values from the discrete set below:

$$\mathrm{pt} \in \left\{ \mathrm{pt}_1 = \mathrm{pt}_{\min}, \mathrm{pt}_2, \ldots, \mathrm{pt}_{N_{\mathrm{pt}}} = \mathrm{pt}_{\max} = T_{\mathrm{env}} \right\} \tag{15}$$

where $\mathrm{pt}_{\min}$ is the minimum feasible placing temperature, N_{pt} is the number of placing temperatures, and $\mathrm{pt}_{\max} = T_{\mathrm{env}}$ is the maximum placing temperature, which corresponds to placing concrete at the ambient temperature (T_{env}).

The height of the lifts (hl). This variable influences the dissipation of the heat generated by the hydration reaction. The shallower the lift, the greater the dissipation of heat before the next lift is placed, and the lower the maximum temperature attained in the structure. On the other hand, the deeper the lifts, the fewer the horizontal construction joints, the shorter the construction period, and the lower the costs. The variable hl is discrete because, in practice, the height of the lifts are usually multiples of a given length due to construction requirements. Since the values of hl are limited by a minimum and maximum feasible height, we can write:

$$\mathrm{hl} \in \{\mathrm{hl}_1 = \mathrm{hl}_{\min}, \mathrm{hl}_2, \ldots, \mathrm{hl}_{\mathrm{Nhl}} = \mathrm{hl}_{\max}\} \tag{16}$$

where Nhl is the number of lift heights, $\mathrm{hl}_{\max}$ is the maximum feasible height of the lifts, and $\mathrm{hl}_{\min}$ is the minimum feasible height of the lifts.

Although it is possible for a construction scheme to use lifts of varying heights, for the sake of simplicity, in this paper all the lifts, except the last, are taken to be the same height. If the division is not exact, the last lift will be the smaller one. Accordingly, the height of the lifts determines the number of lifts, as follows:

$$\begin{aligned} &\mathrm{NL} = \mathrm{HS_t}/\mathrm{hl} \quad \text{if } \mathrm{HS_t}/\mathrm{hl} \text{ is an exact division} \\ &\mathrm{NL} = \mathrm{int}(\mathrm{HS_t}/\mathrm{hl}) + 1 \quad \text{if } \mathrm{HS_t}/\mathrm{hl} \text{ is not exact} \end{aligned} \tag{17}$$

where int represents the integer part of NL and $\mathrm{HS_t}$ is the total height of the structure.

The placing frequency (pf). The extent of heat dissipation in the concrete volume depends on the time period between the construction of one lift and the placing of the next. If this time period increases, the maximum temperature reached in the lift will be lower, but the duration of the construction will be longer, increasing the costs. The variable pf is defined here as the construction frequency, which corresponds to the time spent to place the lift plus the time period until construction of the next lift. It is also, generally, a discrete variable, since the construction frequency is not established on the basis of fractions of days. It is limited by a minimum and maximum feasible placing frequency, as follows:

$$\mathrm{pf} \in \left\{ \mathrm{pf}_1 = \mathrm{pf}_{\min}, \mathrm{pf}_2, \ldots, \mathrm{pf}_{N_{\mathrm{pf}}} = \mathrm{pf}_{\max} \right\} \tag{18}$$

where N_{pf} is the number of placing frequencies, $\mathrm{pf}_{\min}$ and $\mathrm{pf}_{\max}$ being, respectively, the minimum and the maximum placing frequencies as established by the contractor.

The value $\mathrm{pf}_{\min}$ does not correspond to the *crash time* as defined within the framework of a construction time-cost trade-off problem [42], i.e., the minimum feasible duration for a construction activity. Since $\mathrm{pf}_{\min}$ depends on the duration of activities such as the preparation of the horizontal joint and the installation of formwork, it is *crashable* because the contractor may choose different crew sizes, equipment, and construction methods to reduce $\mathrm{pf}_{\min}$ [43], generally at higher costs. The costs of the activities having a duration included in $\mathrm{pf}_{\min}$ are considered to be constants in the optimization problem dealt with in this paper, i.e., these costs do not vary with tc, pt, hl and pf.

Given the number of lifts and the placing frequency, it is possible to calculate the construction time, ct, which may be calculated by formula (19), allowing the minimum amount of time after cooling the last lift to consider the construction to be finished.

$$\mathrm{ct} = (\mathrm{NL} - 1) \cdot \mathrm{pf} + \mathrm{pf}_{\min} \tag{19}$$

From formulas (16)–(19) it can be seen that there is a minimum feasible time $\mathrm{ct}_{\min} = \mathrm{ct}(\mathrm{hl}_{\max}, \mathrm{pf}_{\min})$, and a maximum feasible time $\mathrm{ct}_{\max}(\mathrm{hl}_{\min}, \mathrm{pf}_{\max})$ that define the domain of ct:

$$\mathrm{ct} \in [\mathrm{ct}_{\min}, \mathrm{ct}_{\max}] \tag{20}$$

The vector of variables, designated by $\boldsymbol{x}$, can then be defined as:

$$\boldsymbol{x}^{\mathrm{T}} = \{x_1, x_2, x_3, x_4\} = \{\mathrm{tc}, \mathrm{pt}, \mathrm{hl}, \mathrm{pf}\} \tag{21}$$

4.3. Costs

Since the geometry of the structure is given, the cost function is established for a fixed total volume of concrete $V_{\mathrm{Con,tot}}$, as follows:

$$\begin{aligned} C/V_{\mathrm{Con,tot}} &= c \\ &= (c_{\mathrm{Fixed}} + c_{\mathrm{RM}}(\mathrm{tc}) + c_{\mathrm{CC}}(\mathrm{pt}) + c_{\mathrm{PO}}(\mathrm{hl}, \mathrm{pf})) \end{aligned} \tag{22}$$

where C is the total cost; c is the total unit cost; c_{Fixed} represents all the unit costs that do not vary with hl, pf, tc and pt, such as the cost of plant purchase, installation and other constant costs of the activities related to $\mathrm{pf}_{\min}$;

$c_{RM}(tc)$ is the unit cost of the raw material, which is a function of the type of concrete; $c_{CC}(pt)$ is the unit cost of concrete cooling, which is a function of the placing temperature; and $c_{PO}(hl, pf)$ is the unit cost of plant operation, which varies with the total construction time, which in turn depends on the height of the lifts and the placing frequency. This cost includes leasing and operation of equipment, concrete treatment, consolidation and placing (with the exception of cooling) and so on.

The unit costs are expressed as proportions that indicate their weighting in the total cost. These weights are defined by the coefficients ω as follows:

$$\begin{aligned} &c_{Fixed} = \omega_{Fixed} \cdot c; \quad c_{RM} = \omega_{RM} \cdot c; \\ &c_{CC} = \omega_{CC} \cdot c; \quad c_{PO} \cong \omega_{PO} \cdot c; \\ &\omega_{Fixed+}\omega_{RM+}\omega_{CC+}\omega_{PO} = 1 \end{aligned} \tag{23}$$

The values of these weights depend on factors such as the type of construction, local conditions, variations in the unit costs, etc. However, regardless of the fuzziness of these unit costs, it is always possible to estimate them when a project is being planned. For example, the unit cost of raw material, c_{RM}, can be calculated as follows:

$$\begin{aligned} c_{RM}(tc) = &\sum_{i_B=1}^{n_B tc} c_{B_{i_B,tc}} B_{i_B,tc} + c_W W_{tc} + \sum_{i_P=1}^{n_P tc} c_{P_{i_P,tc}} P_{i_P,tc} \\ &+ \sum_{i_G=1}^{n_G tc} c_{G_{i_G,tc}} G_{i_G,tc} + \sum_{i_A=1}^{n_A tc} c_{A_{i_A,tc}} A_{i_A,tc} \end{aligned} \tag{24}$$

with c_B, c_W, c_P, c_G and c_A being the unit cost of binders, water, pozzolans, aggregates and chemical additives, respectively. If the minimum and maximum cost of the raw material is defined as, respectively, $c_{RM,min}$ and $c_{RM,max}$, we have:

$$c_{RM} \in [c_{RM,min}, c_{RM,max}] \tag{25}$$

The unit cost for cooling the concrete is a function of the placing temperature. For a given problem this function will depend on factors such as the type of building, the availability of an industrial procedure for cooling the material, the place where the plant is installed, the volume of concrete, etc. For example, the construction of a large dam may require an ice plant to be built nearby so that ice can be easily transported to the mixing unit. On the other hand, for the construction of an urban building the engineer might have available commercial ready mix suppliers that would provide the material precooled to the required temperature. Nevertheless, in both cases, the unit costs for cooling the concrete are known to the contractor, and the function relating the placing temperatures to their costs can be determined. This function can have any shape, but it will decrease or remain constant with increasing values of pt. Its range is as follows:

$$c_{CC} \in [c_{CC,min} = 0, c_{CC,max}] \tag{26}$$

where the maximum cost ($c_{CC,max}$) corresponds to the minimum feasible placing temperature (pt_{min}) and the minimum cost ($c_{CC,min} = 0$) corresponds to placing concrete uncooled.

The unit cost for plant operation, $c_{PO} = c_{PO}(hl, pf)$, is determined as a function of the time spent in constructing the whole structure:

$$c_{PO} = c_{PO}(ct(hl, pf)) \tag{27}$$

Briefly, this is the function that relates time to money. The function varies between a minimum cost, $c_{PO,min}$, that corresponds to the minimum feasible time, ct_{min}, and a maximum cost, $c_{PO,max}$, that corresponds to the maximum feasible time ct_{max}:

$$c_{PO} \in [c_{PO,min}, c_{PO,max}] \tag{28}$$

As for the unit cost of cooling concrete, the cost function for plant operation can have any shape, but it will increase or remain constant with increasing values of ct.

4.4. Normalized unit cost, objective function and fitness function

If $\tilde{c}(\boldsymbol{x})$ is defined as the normalized variable unit cost

$$\begin{aligned} &\tilde{c}(\boldsymbol{x}) = \frac{c_{RM}(tc) + c_{CC}(pt) + c_{PO}(hl, pf)}{c_{RM,max} + c_{CC,max} + c_{PO,max}}, \\ &\tilde{c}(\boldsymbol{x}) \in [\tilde{c}_{min}, 1] \end{aligned} \tag{29}$$

where $\tilde{c}_{min}$ is the minimum normalized cost, obtained for $c_{RM} = c_{RM,min}$, $c_{CC} = c_{CC,min}$ and $c_{PO} = c_{PO,min}$, the objective function can be expressed as:

$$f(\boldsymbol{x}) = \tilde{c}(\boldsymbol{x}) \tag{30}$$

If $ECr(\boldsymbol{x}) \in [0, 1]$ is a measure of the extent of cracking, taken in this paper to be the plastified finite elements volume ratio:

$$ECr = \frac{\sum_{i_{el}=1}^{n_{plast}} V_{i_{el}}}{\sum_{i_{el}=1}^{n_{el}} V_{i_{el}}}; \quad \begin{cases} ECr = 0 & \text{for an uncracked structure} \\ 0 < ECr \leqslant 1 & \text{for a cracked structure} \end{cases} \tag{31}$$

where n_{plast} is the number of plastified finite elements, n_{el} is the total number of finite elements, and $V_{i_{el}}$ is the volume of an individual element, the optimization problem can be written as:

$$\begin{aligned} &\text{Minimize } f(\boldsymbol{x}) \\ &\text{Under the constraint defined as } ECr(\boldsymbol{x}) = 0 \end{aligned} \tag{32}$$

The constraint, i.e., the rejection of cracked structures, is handled by a penalty scheme. A fitness function, set out below, is therefore introduced:

$$\begin{aligned} F &= f(\boldsymbol{x}) && \text{for an uncracked structure} \\ F &= f(\boldsymbol{x}) + P(\mathrm{ECr}(\boldsymbol{x}), t) && \text{for a cracked structure} \end{aligned} \tag{33}$$

where the penalty $P(\mathrm{ECr}(\boldsymbol{x}), t)$ is a function of both $\mathrm{ECr}(\boldsymbol{x})$, and t, which represents the generation.

The literature points to several techniques to handle constraints in genetic algorithms. Coello [44] refers to penalty functions, special representations and operators, repair algorithms, separation of objectives and constraints, and hybrid methods. Coello concludes that, in general, the use of simple dynamic or static penalty approaches is recommended for new applications, for the sake of simplicity and efficiency. The robustness and simplicity of static penalties had already been pointed out by Deb [45] and Michalewicz and Scoenauer [46]. Because the research presented in this paper deals with a new optimization problem, a conservative penalty scheme was chosen and a combination of a dynamic penalty for the early generations with a static penalty for the late generations is used. The penalty function is depicted in Fig. 5.

The penalty function is bilinear such that, in the first half of the generations (i.e., until $t = N_g/2$, N_g being the number of generations) the individuals that present cracking under a certain cracking threshold ($\mathrm{ECr}_{\lim}(t)$), are not fully penalized. For generations after $N_g/2$, the penalty becomes static and all cracked structures are penalized by the same value $P(\boldsymbol{x}, t) = 1 - \tilde{c}_{\min}$. The penalty function can be written as follows:

$$P(\mathrm{ECr}(\boldsymbol{x}), t) = \begin{cases} 1 - \tilde{c}_{\min} \\ \quad \text{if } \mathrm{ECr}(\boldsymbol{x}) > \mathrm{ECr}_{\lim}(t) \\ \mathrm{ECr}(\boldsymbol{x}) \frac{1-\tilde{c}_{\min}}{\mathrm{ECr}_{\lim}(t)} \\ \quad \text{if } 0 < \mathrm{ECr}(\boldsymbol{x}) \leqslant \mathrm{ECr}_{\lim}(t) \end{cases} \tag{34}$$

where

$$\mathrm{ECr}_{\lim}(t) = \begin{cases} \mathrm{ECr}_{\lim}(1) - t\frac{\mathrm{ECr}_{\lim}(1)}{(n_g/2)} & \text{if } 1 \leqslant t < (n_g/2) \\ 0 & \text{if } (n_g/2) \leqslant t \leqslant n_g \end{cases} \tag{35}$$

It can be seen from formula (35) that $\mathrm{ECr}_{\lim}(t)$ decreases with a constant time-step for $1 \leqslant t < (n_g/2)$; this constant variation has been chosen for the sake of simplicity.

From formulas (29)–(33) it is clear that for the uncracked solutions, $F \in [\tilde{c}_{\min}, 1]$. When the extent of cracking is equal to or greater than the threshold, the solutions are penalized in such a way that the fitness of the cheaper cracked structure (i.e., $f = \tilde{c}_{\min}$ and $\mathrm{ECr} \geqslant \mathrm{ECr}_{\lim}(t)$) would be equal to or greater than the more expensive uncracked structure (i.e., the structure for which $f = 1$ and $\mathrm{ECr} = 0$). Thus we derive from formula (33) (see also Fig. 5):

$$\begin{aligned} &P(0, t) = 0; \quad P(\mathrm{ECr} \geqslant \mathrm{ECr}_{\lim}(t)) = 1 - \tilde{c}_{\min} \\ &\quad \Rightarrow P(\mathrm{ECr}, t) \in [0, 1 - \tilde{c}_{\min}] \end{aligned} \tag{36}$$

which results in the following considerations regarding the fitness function:

$$\begin{aligned} F &= \underbrace{\tilde{c}_{\min}}_{f} + \underbrace{1 - \tilde{c}_{\min}}_{P} = 1 && \text{for the cheaper structure, cracked beyond the threshold} \\ F &= \underbrace{1}_{f} + \underbrace{0}_{P} = 1 && \text{for the more expensive uncracked structure} \\ F &= \underbrace{1}_{f} + \underbrace{1 - \tilde{c}_{\min}}_{P} = 2 - \tilde{c}_{\min} && \text{for the more expensive structure, cracked beyond the threshold} \end{aligned} \tag{37}$$

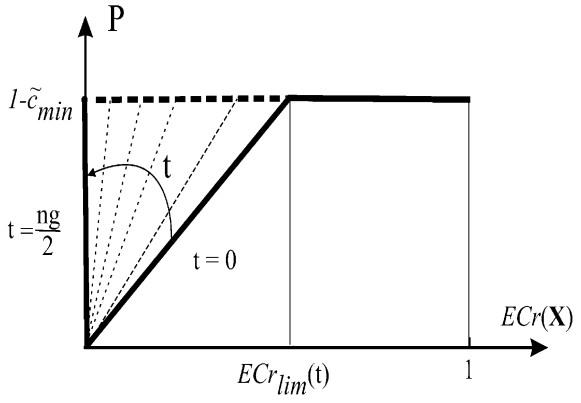

Fig. 5. Penalty function.

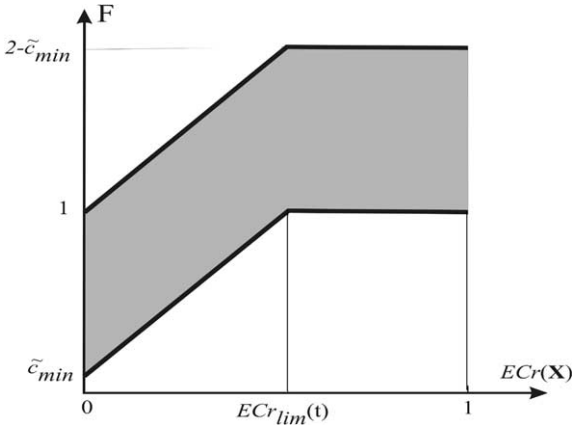

Fig. 6. Fitness function.

The fitness function, F, is shown in Fig. 6, which illustrates the scheme of constraint handling. It can be seen from Fig. 6 that $F \in [\tilde{c}_{\min}, 1]$ for uncracked structures; $F \in [\tilde{c}_{\min}, 2 - \tilde{c}_{\min}]$ for structures cracked beneath the threshold; and $F \in [1, 2 - \tilde{c}_{\min}]$ for structures cracked beyond the threshold.

5. Example

This section presents an application of the proposed optimizing procedure: the construction of a concrete dam for a small hydropower plant.

The concrete dam is 10 m high and its total concrete volume is 3000 m^3. It is a typical project, taken from the Brazilian Manual of Small Hydropower Plants Study and Design [47]. The main geometric characteristics and the finite element mesh used for the following simulations are shown in Fig. 7.

5.1. Design variables

The design variables, as defined in Section 4, are described below:

Type of concrete (tc): Eight types of concretes were used, all taken from FURNAS concrete laboratory data

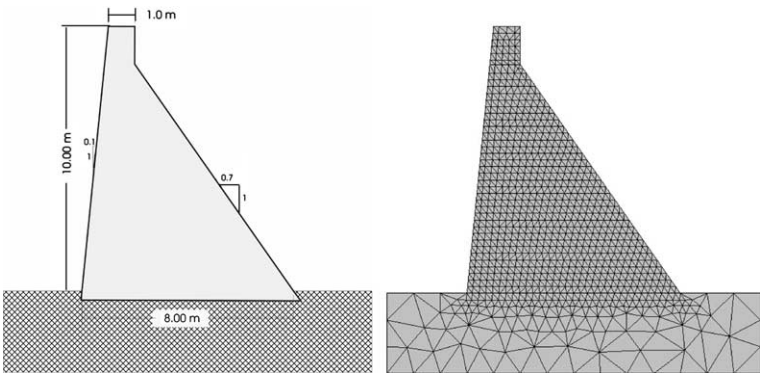

Fig. 7. Geometric characteristics of the dam and finite element mesh.

Table 1
Composition of the eight types of concretes

tc	B_1 (cement) (kg/m^3)	B_2 (fly ash) (kg/m^3)	B_3 (slag) (kg/m^3)	W (kg/m^3)	G_1 (fine) (kg/m^3)	G_2 (coarse) (kg/m^3)
1	139		170	165	626	1318
2	338	57		190	664	1057
3	299	50		187	700	1068
4	336			185	745	1090
5	335			160	603	1197
6	323			178	852	1084
7	127		237	163	655	1165
8	239		80	171	621	1303

Table 2
Thermo-chemo-mechanical parameters for the eight types of concretes[a]

tc	C_ε (J kg/K)	k W/(m K)	α (10^{-6})	$f_{c,\infty}$ (MPa)	E_∞ (MPa)	ε_∞^{sh} (10^{-6})[a]
1	1017	2.65	13.02	29.9	21.7	23.46
2	1109	2.64	10.78	28.9	30.6	21.09
3	1134	2.64	10.37	24.8	25.9	11.37
4	1084	2.64	10.62	30.2	26.0	24.17
5	1059	2.64	12.03	27.3	22.4	17.30
6	1092	2.24	9.93	23.9	23.2	10.05
7	1063	2.26	12.58	25.4	24.0	12.79
8	1050	2.49	12.09	25.2	17.1	12.32

[a] Given by the model of Le Roy et al. [49].

bank [48]. FURNAS is the electrical energy generation and distribution company in the south east of Brazil. The variable tc is thus defined as $\mathrm{tc} \in \{1, 2, \ldots, 8\}$. The composition of these types of concretes is given in Table 1 and their thermo-chemo-mechanical parameters are given in Table 2. The activation energy and the parameter ξ_0 were considered to be constant for all the materials, reading, respectively, $E_a/R(1, \ldots, 8) = 4000/\mathrm{K}$ and $\xi_0(1, \ldots, 8) = 0.1$. The curves of the adiabatic temperature rise are given in Fig. 8 and the curves of the normalized affinity are given in Fig. 9.

Placing temperature (pt): This variable is defined as $\mathrm{pt}(^\circ\mathrm{C}) \in \{10, 11, 12, 13, 14, 15, 16, 17, 18, 19, 20, 21, 22, 23, 24, 25\}$, where 10 °C is the minimum cooling temperature available for the present application, and 25 °C is the average ambient temperature.

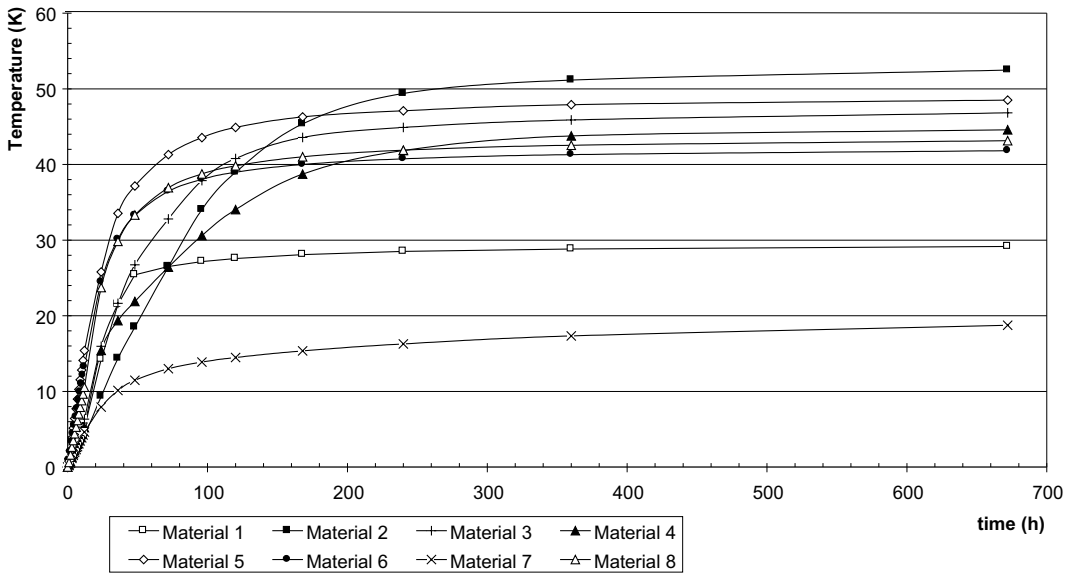

Fig. 8. Adiabatic temperature rise for the eight types of concretes.

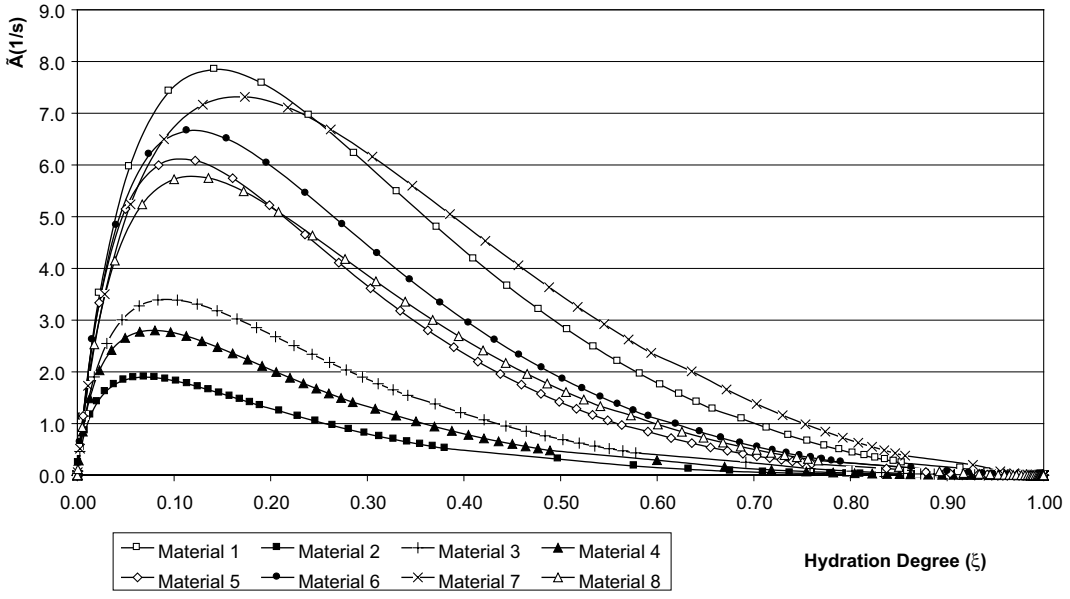

Fig. 9. Affinity curves $\widetilde{A}(\xi)$ for the eight types of concretes.

Table 3
Estimated unitary costs for the components of concrete

Component	Unitary cost (US$/kg)
Cement	0.077
Fly ash	0.033
Ground granulated blast furnace slag	0.033
Aggregate	0.0077
Water	0.0077

Table 4
Unitary costs of the concretes

tc	c_{RM} (US$/m^3)
1	24.08
2	34.93
3	30.88
4	34.51
5	34.60
6	33.11
7	26.73
8	27.96

Height of the lifts (hl): The values used in the present application are $\mathrm{hl}(m) \in \{0.5, 0.75, 1.0, 1.25, 1.5, 1.75, 2.0, 2.5\}$, with each value producing a corresponding number of lifts (see formula (17)) $\mathrm{NL} \in \{20, 14, 10, 8, 7, 6, 5, 4\}$.

Placing frequency (pf): This variable was given a range of values $\mathrm{pf(days)} \in \{6, 7, 8, 9, 10, 11, 12, 13, 14, 15, 16, 17, 18, 19, 20, 21\}$. A minimum value of 6 days was chosen because it was assumed that 5 days is the minimum period of time needed to cure the concrete and prepare the horizontal joint and the formwork for the new lift.

Given the limit values adopted for hl and pf, construction time ct, computed using formula (19), can vary between 24 and 405 days.

5.2. Costs

In this example, the weighting of the cost components, as defined by formulas (23), was assumed to be,

Table 5
Unitary costs for cooling concrete

pt (°C)	c_{CC} (US$/kg)
10	21.88
11	18.75
12	16.25
13	14.38
14	12.81
15	11.25
16	9.38
17	8.13
18	6.88
19	5.63
20	4.38
21	3.13
22	1.88
23	0.94
24	0.31
25	0.00

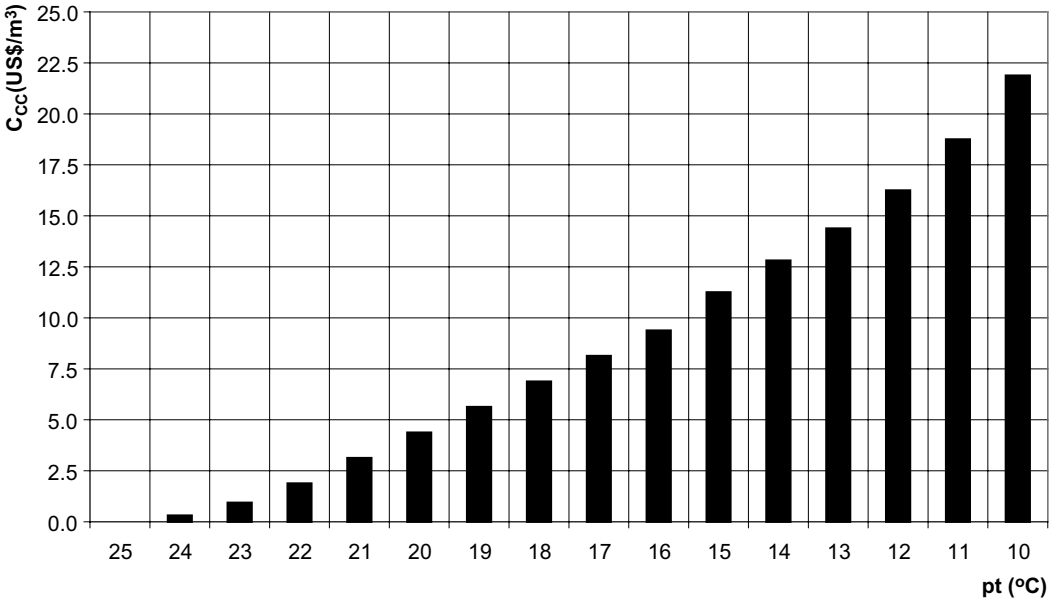

Fig. 10. Function $c_{CC}(\mathrm{pt})$.

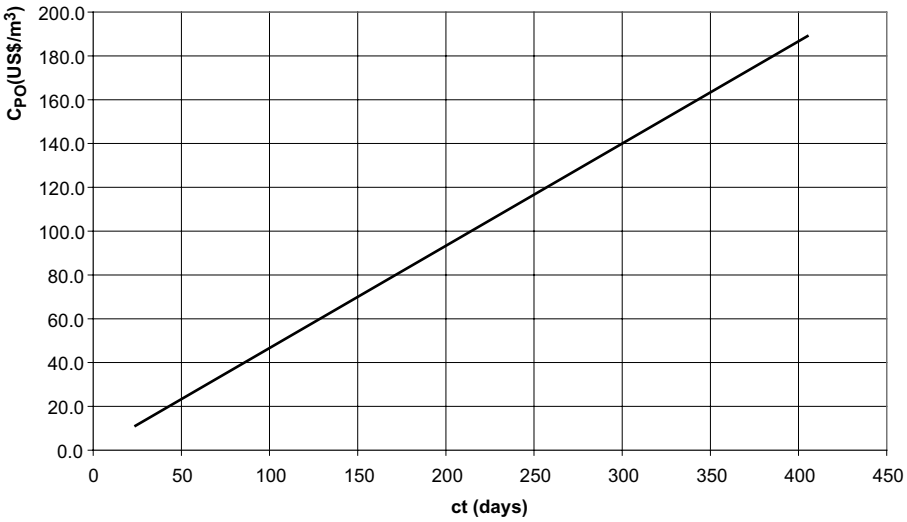

Fig. 11. Function $c_{PO}(ct)$.

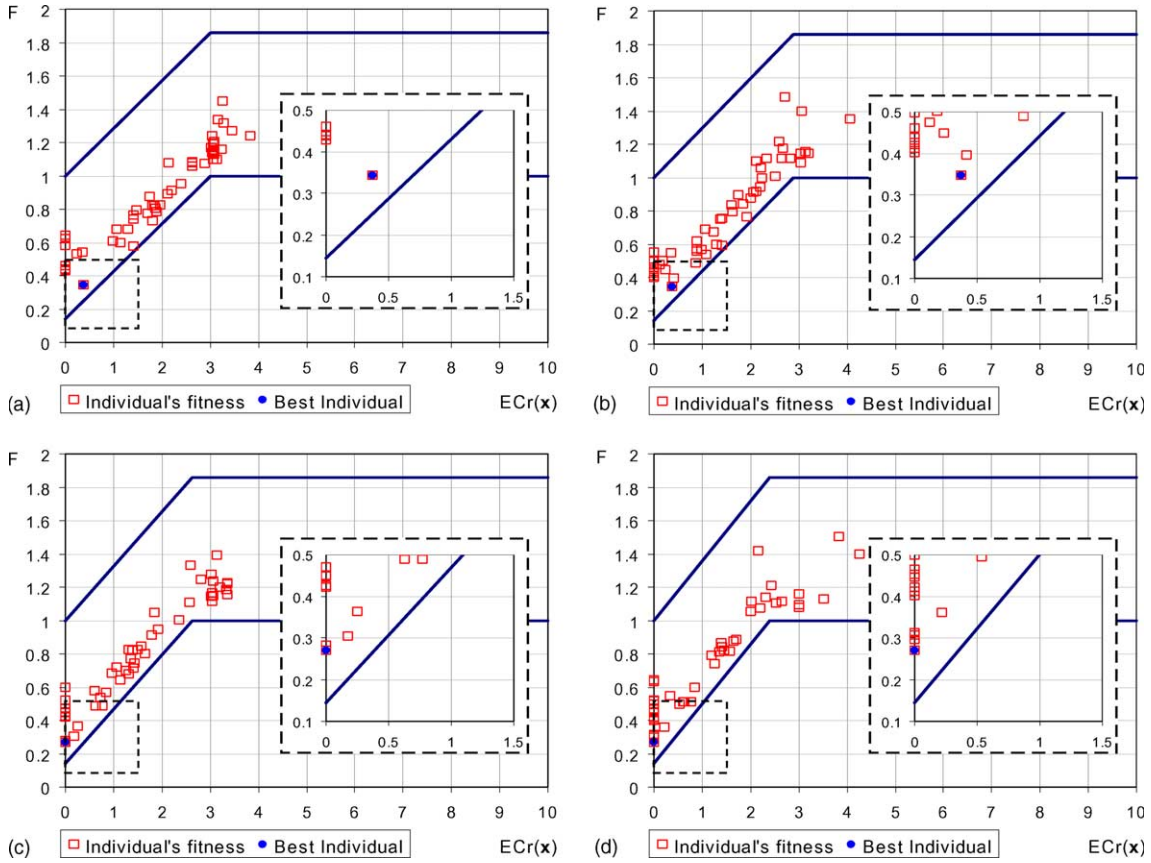

Fig. 12. Evolution of the generations: (a) initial population, (b) 1st generation, (c) 3rd generation, (d) 5th generation, (e) 10th generation, (f) 15th generation, (g) 25th generation, (h) 50th generation.

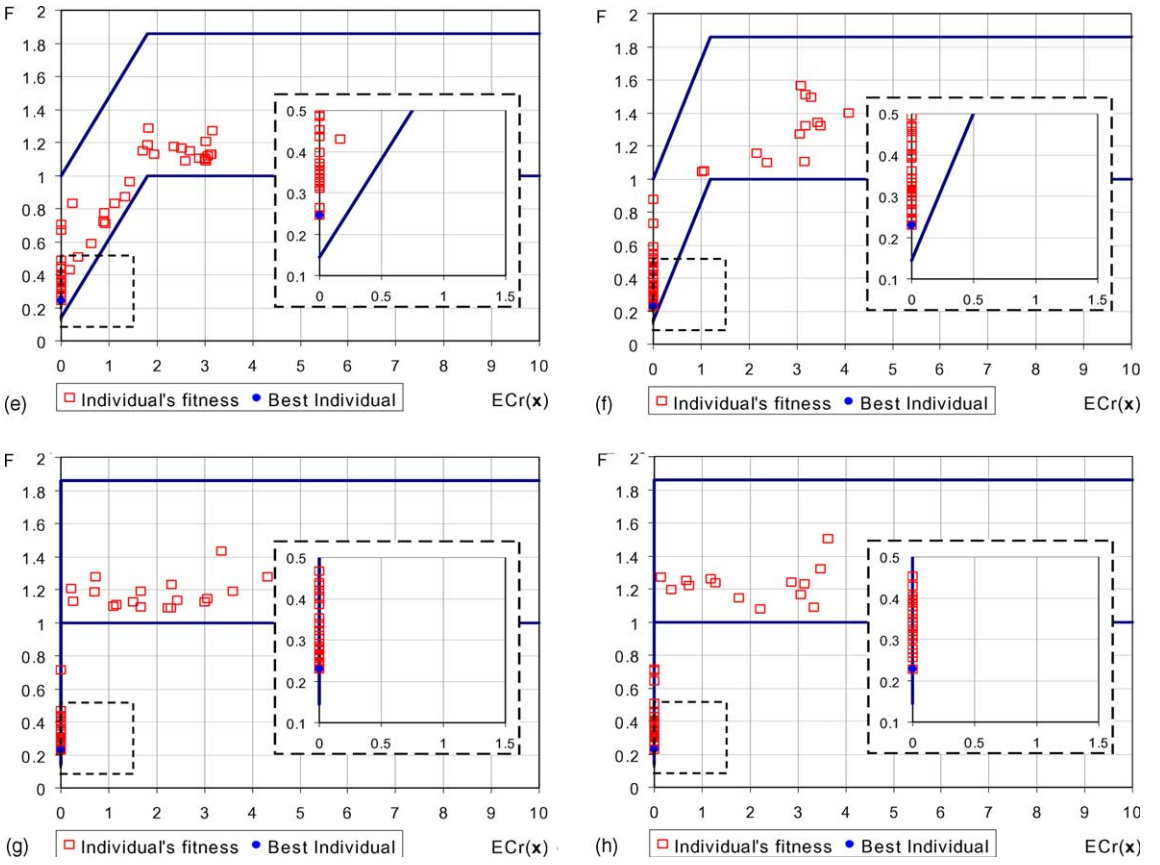

Fig. 12 (*continued*)

on average $\omega_{\text{Fixed}} = 35\%$; $\omega_{\text{RM}} = 30\%$; $\omega_{\text{CC}} = 5\%$; and $\omega_{\text{PO}} = 30\%$.

The unit costs $c_{\text{RM}}(\text{tc})$, for the several types of concrete, are calculated using formula (24) using the quantities of raw material shown in Table 1 and assuming that the unit cost of the components is that given in Table 3. The results are shown in Table 4, from which it can be deduced that the minimum and maximum costs are $c_{\text{RM,min}} = 24.08$ US\$/m^3 and $c_{\text{RM,max}} = 34.60$ US\$/m^3.

The function depicted in Fig. 10 was used to calculate the unit cost $c_{\text{CC}}(\text{pt})$. Based on field experience, this function reflects the fact that the relationship between the cost of cooling concrete and the placing temperature is not linear. The computed values for $c_{\text{CC}}(\text{pt})$ are given in Table 5, where it can be seen that $c_{\text{CC,min}} = 0.0$ US\$/m^3 and $c_{\text{CC,max}} = 21.88$ US\$/m^3.

The unit cost $c_{\text{PO}}(\text{ct}(\text{hl}, \text{pf}))$ is calculated using the function depicted in Fig. 11, based on the assumption that the relationship between the cost of plant operation and construction time is linear. The minimum and maximum costs are $c_{\text{PO,min}} = 11.2$ US\$/m^3 and $c_{\text{PO,max}} = 189.00$ US\$/m^3.

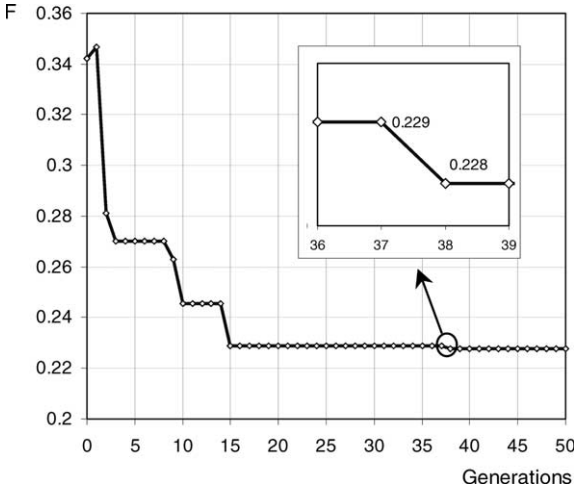

Fig. 13. Evolution of fitness of the best individual.

With the values presented above, $\tilde{c}_{\text{min}}$ is determined to be 0.144, using formula (29).

5.3. Penalty function and genetic algorithm parameters

The first cracking threshold for the penalty function was established as $ECr_{lim}(1) = 0.03$. This value, which was chosen on the basis of experience, indicates that first generation individuals with cracking of less than 3% are not discarded from the evolutionary process. If the cracking exceeds the threshold, the finite element calculation for the individual is terminated, because penalty applied is the same for $ECr_{lim} < ECr \leqslant 100\%$.

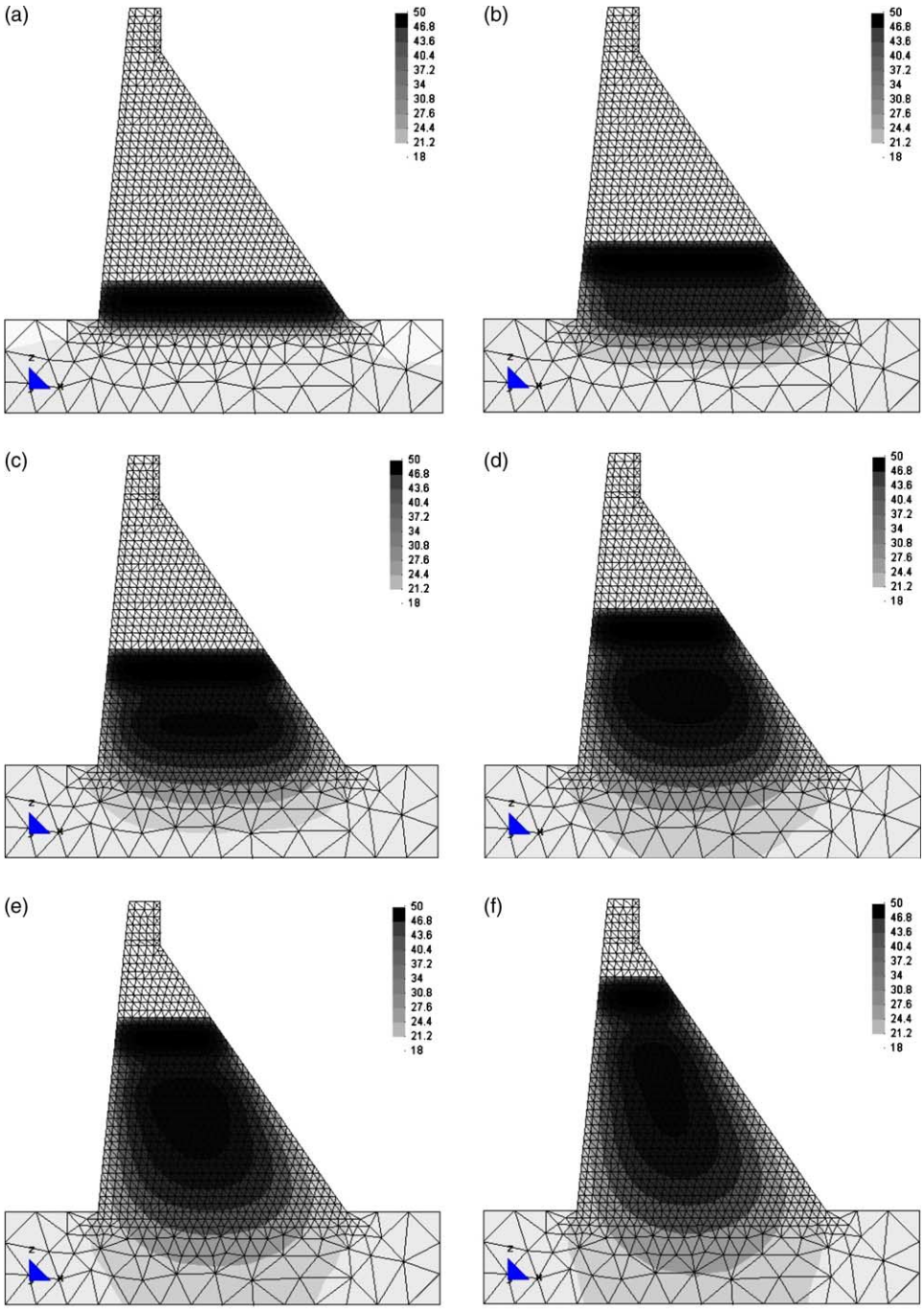

Fig. 14. Temperature fields: (a) 2 days, (b) 7 days, (c) 12 days, (d) 17 days, (e) 22 days, (f) 27 days.

The control parameters of the genetic algorithm set at $N = 50$ individuals, $N_t = 5$ individuals, $P_c = 90\%$ and $P_m = 5\%$. The algorithm terminates when the maximum number of generations is reached ($N_g = 50$).

6. Results

Fig. 12 shows the evolution of the generations in terms of extent of cracking and individual fitness.

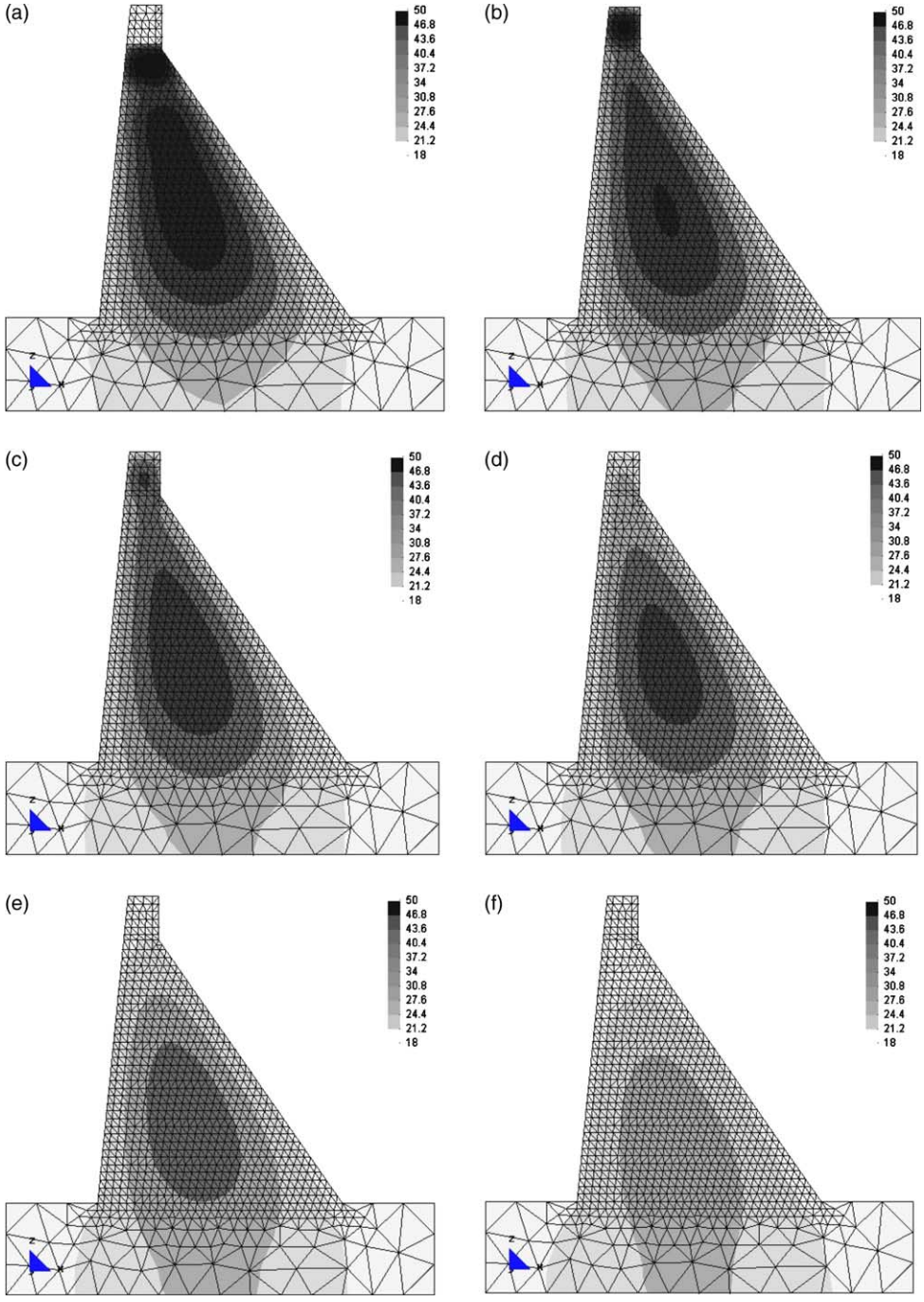

Fig. 15. Temperature fields: (a) 32 days, (b) 37 days, (c) 39 days, (d) 42 days, (e) 49 days, (f) 63 days.

Significant diversity can be seen in the initial population, where several individuals present cracking. In the initial population and the first generation, the fittest individual was found within the cracked domain, while from the second generation on the best individual was an uncracked structure. It can also be observed that the number of uncracked individuals increases with the evolution of the generations.

Fig. 13 shows the evolution of the fittest individual. From this figure we can conclude that the use of a

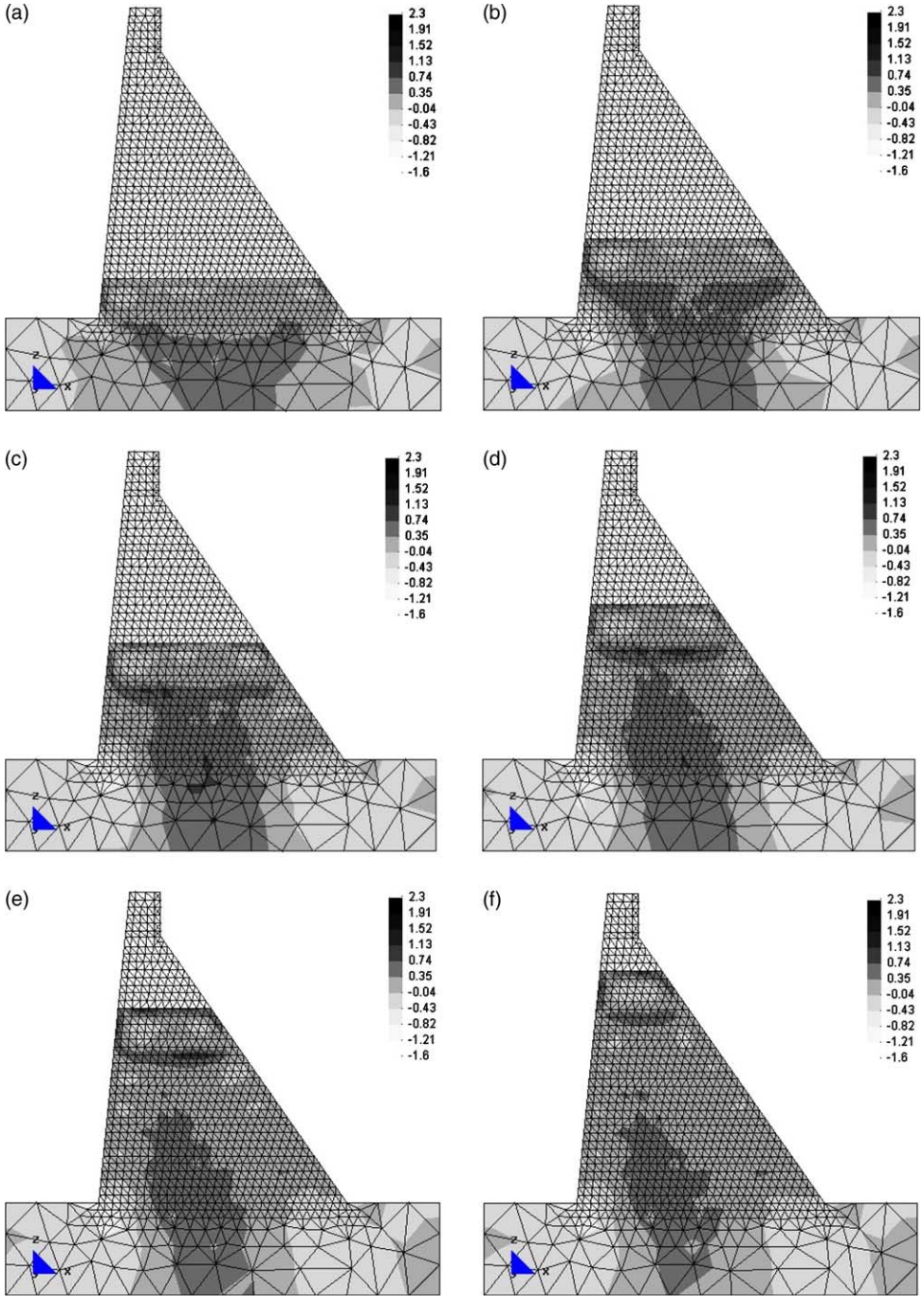

Fig. 16. Principal stress fields: (a) 2 days, (b) 7 days, (c) 12 days, (d) 17 days, (e) 22 days, (f) 27 days.

penalty function that allows for a certain amount of cracking in the first generations was effective in avoiding stagnation in the evolutionary process.

The analysis was carried out using a 1.8 GHz/1GB Personal Computer. Considering that the design variables change for each individual, the computer time required to run the FEM analysis of one individual was not constant. The computer time is mainly dependent on the number of lifts and placing frequency that define the construction process. Other important aspect is the cracking extension, since the analysis for each individual stops when the cracking threshold is reached. Therefore,

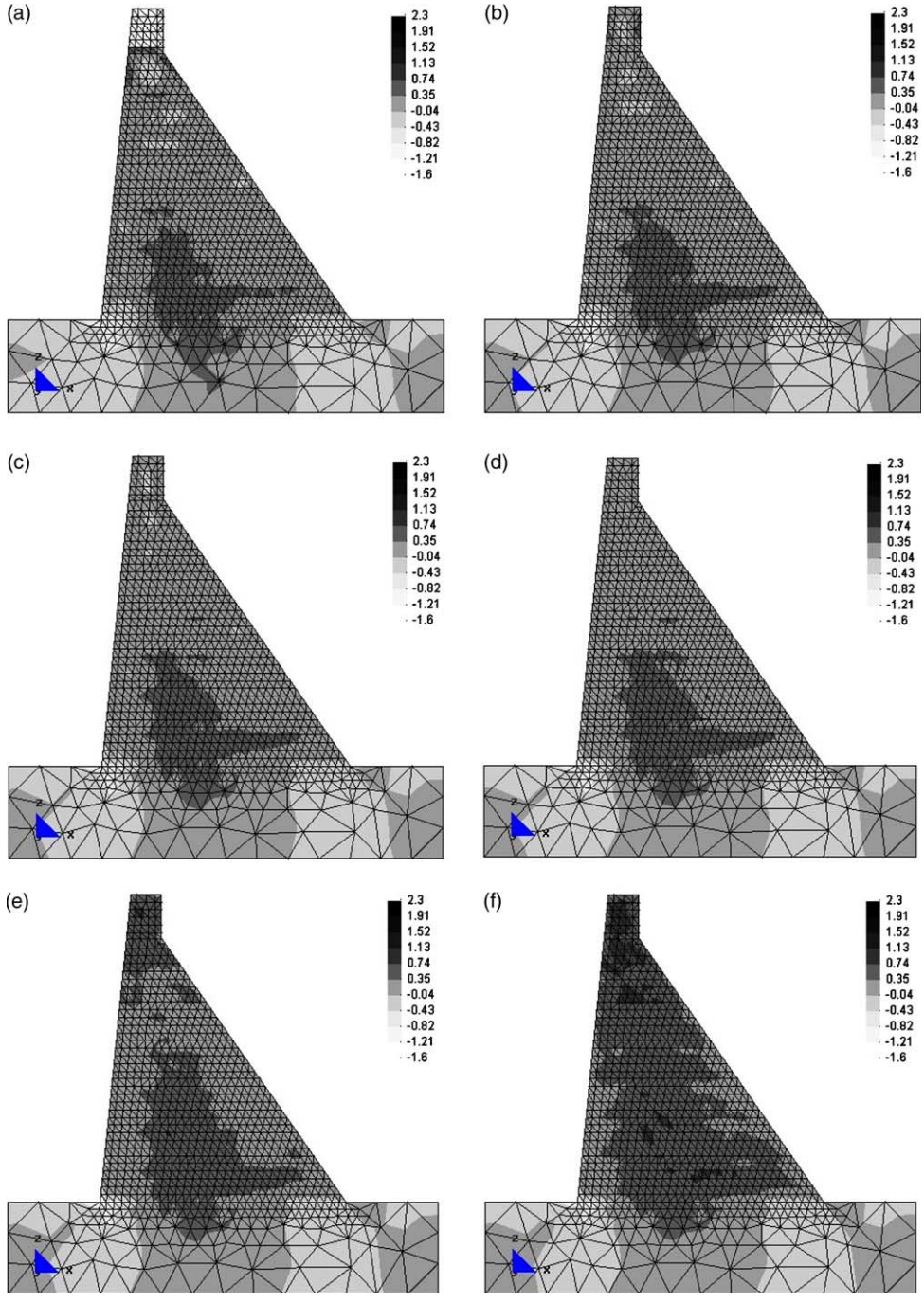

Fig. 17. Principal stress fields: (a) 32 days, (b) 37 days, (c) 39 days, (d) 42 days, (e) 49 days, (f) 63 days.

the computer time spent to run the analysis of each individual ranged from 1 to 30 min. To have the full analysis completed (50 generations) the average computer time was about 300 h.

The analysis showed that the minimum cost is attained with a construction scheme described by the following optimal values:

$$tc = 8; \quad pt = 19\ ^{\circ}C; \quad hl = 1.25\ m; \quad pf = 5\ days \quad (ct = 48\ days)$$

Some results obtained for this optimal set are given in Fig. 14, Fig. 15 (temperature fields for several construction steps), Figs. 16 and 17 (principal stress fields for several construction steps).

7. Conclusions

This paper presents a new procedure that can help the engineer in deciding on the construction process and in choosing the composition of mass concrete structures. The procedure combines an advanced thermo-chemo-mechanical model and optimization techniques based on genetic algorithms. The procedure was applied to optimize the hypothetical construction of a small concrete dam and the results indicated that the use of the cost optimization procedure can result in substantial savings.

The procedure can readily be applied to the actual design of massive structures in which early age cracking is a predominant design constraint. The principal application of the procedure would therefore be in the optimization of concrete dams, massive foundation slabs and bridge decks and other structures made of high performance concretes for which autogenous shrinkage coupled with thermal stresses is a major concern.

The unit costs functions for the design variables are discrete and can be adapted in practice to any massive construction, as long as the effective costs for the construction and materials are known.

Because this is a computer-intensive method, the next steps in the refining of the procedure would be to optimize the computational implementation to permit analysis of larger structures through complex 3D geometries.

Acknowledgements

This research is supported by NSF-CNPq grant for collaborative research between MIT and COPPE/Universidade Federal do Rio de Janeiro, Brazil, on high performance computing applied to the modeling of concrete dams. The authors gratefully acknowledge the support of this work by CNPq and NSF.

References

[1] Springenschmid R, editor. Thermal cracking in concrete at early ages, Proceedings of the RILEM International Symposium, Munich, October 1994. London: E&FN Spon; 1995.

[2] Springenschmid R, editor. Prevention of thermal cracking in concrete at early ages, State of the art report prepared by RILEM TC 119. London: E&FN Spon; 1998.

[3] Jansen RB, editor. Advanced dam engineering for design, construction and rehabilitation. New York: Van Nostrand Reinhold; 1988.

[4] Fairbairn EMR, Silvoso MM, Alves JLD, Tolêdo Filho RD. Optimization of mass concrete construction using genetic algorithms. In: Proceedings of the 15th Engineering Mechanics Conference, New York, June 2002, CD-ROM. p. 1–8.

[5] ICOLD (International Commission on Large Dams), Concrete dams—Control and treatment of cracks—review and case histories, Bulletin 107. ICOLD, Paris, 1997.

[6] ACI Committe 207, Mass concrete. American Concrete Institute, Michigan, 1996.

[7] ACI Committe 207, Effect of restraint, volume change, and reinforcement on cracking of mass concrete. American Concrete Institute, Michigan, 1995.

[8] Gadja J, Vangeem M. Controlling temperatures in mass concrete. Concrete International 2002;24:59–62.

[9] Emborg M. Models and methods for computation of thermal stresses. In: Springenschmid R, editor. Prevention of thermal cracking in concrete at early age. London: E&FN Spon; 1998. p. 178–230.

[10] Fairbairn EMR. The Brazilian experience on the use of Maxwell chain model for solving the thermo-mechanical problem of concrete dams. In: Annales de l'ITBTP, 520 série: théorie et méthodes de calcul 343, 1994. p. 150–79 (in French).

[11] Luna R, Wu Y. Simulation of temperature and stress fields during RCC dam construction. ASCE J Construct Eng Manage 2000;126:381–8.

[12] Cervera M, Oliver J, Prato T. Simulation of construction of RCC dams. I: Temperature and aging. II Stress and damage. ASCE J Struct Eng 2000;126:1053–69.

[13] CBGB (Brazilian Committee on Large Dams), ELETROBRAS and IBRACON (Brazilian Concrete Institute), Mass concrete in Brazil—technical memory, historical archive. Memória da Eletricidade, Rio de Janeiro, 1989 (in Portuguese).

[14] Sarma KC, Adeli H. Cost optimization of concrete structures. ASCE J Struct Eng 1998;124:570–8.

[15] Ulm F-J, Coussy O. Modeling of thermochemomechanical couplings of concrete at early ages. ASCE J Eng Mech 1995;121:785–94.

[16] Ulm F-J, Coussy O. Strength growth as chemo-plastic hardening in early age concrete. ASCE J Eng Mech 1996;122:1123–32.

[17] Silvoso MM. Optimization of the constructive phase of concrete structures in face to the effects of hydration by genetic algorithms. PhD thesis, COPPE/The Federal University of Rio de Janeiro, Rio de Janeiro, 2003 (in Portuguese).

[18] Castro RE. Multi-objective optimization with genetic algorithms. PhD thesis, COPPE/The Federal University of Rio de Janeiro, Rio de Janeiro, 2001 (in Portuguese).
[19] Ulm F-J, Coussy O. Couplings in early-age concrete: from material modeling to structural design. International Journal of Solids and Structures 1998;35:4295–311.
[20] Ulm F-J, Coussy O, Bazant ZP. The "Chunnel" fire. I: chemoplastic softening in rapidly heated concrete. II: Analysis of concrete damage. ASCE J Eng Mech 1999; 125:272–89.
[21] Hellmich C, Mang HA, Ulm F-J. Hybrid method for quantification of stress states in shotcrete tunnel shells: combination of 3D in situ displacement measurements and thermochemoplastic material law. Comput Struct 2001; 79:2103–15.
[22] Nanakorn P, Meesomklin K. An adaptive penalty function in genetic algorithms for structural design optimization. Comput Struct 2001;79:2257–539.
[23] Pezeshk S, Camp CV, Chen D. Design of nonlinear framed structures using genetic optimization. ASCE J Struct Eng 2000;126:382–8.
[24] Kameshki ES, Saka MP. Optimum design of nonlinear steel frames with semi-rigid connections using a genetic algorithm. Comput Struct 2001;79:1593–604.
[25] Erbatur F, Hasançebi O, Tütüncü I, Kiliç H. Optimal design of planar and space structures with genetic algorithms. Comput Struct 2000;75:209–24.
[26] Rajeev S, Krishnamoorthy CS. Genetic algorithms-based methodologies for design optimization of trusses. ASCE J Struct Eng 1997;123:350–8.
[27] Sarma KC, Adeli H. Fuzzy genetic algorithm for optimization of steel structures. ASCE J Struct Eng 2000; 126:596–604.
[28] Rajan SD. Sizing, shape and topology design optimization of trusses using genetic algorithm. ASCE J Struct Eng 1995;121:1480–7.
[29] Coello CA, Christiansen AD. Multiobjective optimization of trusses using genetic algorithms. Comput Struct 2000; 75:647–60.
[30] Jakiela MJ, Chapman JD, Adewuya A, Saitou K. Continuum structural topology design with genetic algorithm. Comput Methods Appl Mech Eng 2000;186:339–56.
[31] Hadi MNS, Arfiadi Y. Optimum rigid pavement design by genetic algorithms. Comput Struct 2001;79:1617–24.
[32] Friswell MI, Penny JET, Garvey SD. A combined genetic and eigensensitivity algorithm for the location of damage in structures. Comput Struct 1998;69:547–56.
[33] António CAC. A hierarchical genetic algorithm for reliability based design of geometrically non-linear composite structures. Compos Struct 2001;54:37–47.
[34] Nakanishi Y. Application of homology theory to topology optimization of three-dimensional structures using genetic algorithm. Comput Methods Appl Mech Eng 2001;190: 3849–63.
[35] Simo J, Hughes T. Computational inelasticity. Berlin: Springer; 1998.
[36] Ferreira IA. Numerical modeling of thermo-chemo-mechanical couplings in early age concrete. MSc thesis, COPPE/The Federal University of Rio de Janeiro, Rio de Janeiro, 1998.
[37] Helmich C. Shotcrete as part of the new Austrian tunneling method: from thermochemomechanical material modeling to structural analysis and safety assessment of tunnels. PhD thesis, Technischen Universität Wien, Wien, 1999.
[38] Laplante P. Propriétés méchaniques des bétons durcissants: analyse comparée des bétons classiques et à très hautes performances. PhD thesis, École Nationale des Ponts et Chaussées, Paris, France, 1993.
[39] Acker P. Comportement mécanique du béton: apports de l'approche physico-chimique. Res. Rep. LCPC 152, LCPC—Laboratoire Central des Ponts et Chaussées, Paris, 1988.
[40] Byfors J. Plain concrete at early ages. Technical report S-100 44, Swedish Cement and Concrete Research Institute, Stockholm, 1980.
[41] Blickle T, Thiele L. A comparison of selection schemes used in evolutionary algorithms. Evolution Comput 1996; 4-4:361–94.
[42] Li H, Love P. Using improved genetic algorithms to facilitate time-cost optimization. ASCE J Construct Eng Manage 1997;123:233–7.
[43] Liu L, Burns SA, Feng C-F. Construction time-cost trade-off analysis using LP/IP hybrid method. ASCE J Construct Eng Manage 1994;121:446–54.
[44] Coello CAC. Theoretical and numerical constraint-handling techniques used with evolutionary algorithms: a survey of the state of the art. Comput Methods Appl Mech Eng 2002;191:1245–87.
[45] Deb K. An efficient constraint handling method for genetic algorithms. Comput Methods Appl Mech Eng 2000; 186:311–38.
[46] Michalewicz Z, Scoenauer M. Evolutionary algorithms for constrained parameter optimization problems. Evolution Comput 1996;4:1–32.
[47] ELETROBRAS, Manual of small hydropower plants study and design. ELETROBRAS, Brazil, 2000, CD-ROM (in Portuguese).
[48] Andrade WP. Concretes: mass, structural, shot and roller compacted. PINI, São Paulo, Brazil, 1997 (in Portuguese).
[49] Le Roy R, de Larrard F, Pons G. The AFREM code type model for creep and shrinkage of high-performance concrete. In: Proceedings of the IV Int. Syposium on Utilization of High-Strength/High-Performance Concrete, Paris, France, May 1996. p. 387–96.
[50] Coutinho ALGA, Martins MAD, Alves JLD, Landau L, Moraes A. Edge-based finite element techniques for nonlinear solid mechanics problems. International Journal for Numerical Methods in Engineering 2001;50:2053–68.